FULL PAPER *Surgery*

Prevention of Biofilm Formation with a Coating of 2-Methacryloyloxyethyl Phosphorylcholine Polymer

Kiyohisa FUJII[1], Hiroko N. MATSUMOTO[1], Yoshihisa KOYAMA[1], Yasuhiko IWASAKI[1], Kazuhiko ISHIHARA[2] and Kazuo TAKAKUDA[1]*

[1]*Institute of Biomaterials and Bioengineering, Tokyo Medical and Dental University, 2–3–10 Kanda-Surugadai, Chiyoda-ku, Tokyo 101–0062 and* [2]*Department of Materials Engineering, School of Engineering, The University of Tokyo, 7–3–1 Hongou, Bunkyou-ku, Tokyo 113–8656, Japan*

(Received 27 June 2007/Accepted 19 October 2007)

ABSTRACT. Device-associated infections are serious complications, and their prevention is an issue of considerable importance. Since biofilms are responsible for these refractory infections, effective methods to inhibit biofilm formation are required. In this investigation, stainless steel plates with and without 2-methacryloyloxyethyl phosphorylcholine (MPC) polymer, i.e., poly (MPC-co-n-butyl methacrylate) (PMB) coating, were incubated in a medium containing bacteria. In the course of incubation, half of the specimens received antibiotics. The specimens were stained for nucleic acid and polysaccharides, and then examined with a confocal laser scanning microscope. The numbers of bacteria on the specimen surfaces were evaluated by an ATP assay. On the surfaces of the specimens without PMB coating, the formation of a biofilm enveloping bacteria was confirmed. The addition of antibiotics did not effectively decrease the number of bacteria. On the other hand, on the surfaces of the specimens with PMB coating, no biofilm formation was observed, and the number of bacteria was significantly decreased. The addition of potent antibiotics further decreased the number of bacteria by 1/100 to 1/1000 times. The PMB coating combined with the validated use of antibiotics might provide a method for the simultaneous achievement of biocompatible surfaces of devices and the prevention of device-associated infections.

KEY WORDS: biofilm, biomaterials, device-associated infection, MPC, PMB coating.

J. Vet. Med. Sci. 70(2): 167–173, 2008

Device-associated infections are serious complications in patients receiving indwelling catheters. These complications, however, do not limited in such cases; device-associated infections are consistent risk accompanying the usage of any artificial devices. For instance, applications of bone fixation plates to open fractures are contraindicated. Actually, the rate of the infections was reported to be as high as 15% to 18% [23] if an aseptic condition was not maintained during the treatment. Although the microorganisms responsible for these infections are usually indigenous bacteria such as *Staphylococcus epidermidis*, a difficulty arises as antibacterial agents are not effective against these infections. Once the infections are established, persistent inflammations continue as long as the devices remain in the body.

Device-associated infections are caused by bacteria that adhere to the surfaces of internal prosthetic devices and are thought to develop through the following sequence of events [3, 7, 10, 18, 22]. Immediately after the implantation of devices into patients, various molecules such as peptides and proteins are adsorbed onto the surfaces of the materials. These molecules mediate the attachment of bacteria. Once the bacteria, e.g., those belonging to the species *S. epidermidis*, are attached to the surfaces of devices, they proliferate and aggregate there to form biofilms in which the bacteria are enveloped in a thin layer of polysaccharides. The bacteria in the biofilms are protected from the biological defense mechanism, including phagocytosis by macrophages and immunological responses, as well as antibacterial agents for therapeutic use. Hence, the formation of biofilms on the surface of devices establishes refractory infections, i.e., device-associated infections [6, 8, 19, 24, 27, 28].

Various strategies were proposed and are expected to be effective in preventing device-associated infections. Wassall [31] utilized silver coating on stainless steel pins for external skeletal fixation and reported successful infection control. Takahashi [29] developed antibacterial catheters coated with citrate silver and lecithin and reported that biofilm formations were prevented. In these reports, silver coating that has an antibacterial effect was utilized; however, silver is not a biocompatible material and might exert adverse effects on living tissues. It is desirable to realize another approach in which only biocompatible materials are utilized for preventing device-associated infections.

2-Methacryloyloxyethyl phosphorylcholine (MPC) was designed taking into account the surface structure of the biomembrane. MPC polymers have a surface that resists nonspecific protein adsorption and cell adhesion [13–17, 25]. It has been attracting considerable attention for its remarkable antithrombogenicity and has been applied successfully to artificial blood vessels, implantable artificial hearts and artificial lungs. The MPC polymer coating renders the surfaces extremely hydrophilic, prevents the adhesion of proteins, and inhibits the adhesion of platelets. Noting the similarity of platelet adhesion and bacterial adhesions, we might expect that the MPC polymer coating also leads to the inhibition of bacterial adhesion and the forma-

* CORRESPONDENCE TO: TAKAKUDA, K.., Institute of Biomaterials and Bioengineering, Tokyo Medical and Dental University, 2–3–10 Kanda-Surugadai, Chiyoda-ku, Tokyo 101–0062, Japan.
e-mail: takakuda.mech@tmd.ac.jp

tion of biofilm. In fact, Hirota *et al.* [9] had coated coverslips made of polyethylenetelephthalate with MPC polymer and observed decreased adhesion of bacteria to the coverslip surfaces. In their experiments, however, they exposed the specimens to bacteria for only 1 hr and counted the number of bacteria attached to the specimens during this period. In order to elucidate whether MPC polymer coating prevents biofilm formation, a comparative study concerning biofilm formation on noncoated and MPC polymer-coated surfaces, which requires a longer period of exposure to bacteria, should be conducted. Hence, in this investigation, we carried out biofilm formation experiments with both surfaces and examined how MPC polymer, i.e., poly[MPC-co-n-butyl methacrylate (BMA)] (PMB) coating inhibits the formation of biofilms.

MATERIALS AND METHODS

Plate specimens: Stainless steel plates (SUS316L; Nilaco Corp., Tokyo, Japan) with a thickness of 0.1 mm and dimensions of 5 × 5 × 0.1 mm were prepared. The composition of this material was standardized for medical use such as bone fixation devices. Since surface characteristics as bacterial adhesion were examined in this experiment, thin plates of 0.1-mm thickness were adopted for the sake of convenience in cultivation. The specimens were cleaned with acetone, washed with distilled water, and autoclaved at 121°C for 20 min. Further operations with the specimens were carried out in sterile conditions.

Coating with MPC polymer: The MPC was synthesized as previously reported [14]. The PMB was synthesized by radical polymerization of desired amount of MPC and n-butyl methacrylate in ethanol using 2,2'-azobisisobutyronitrile (AIBN) as an initiator [16]. The chemical structure of the PMB was determined by ^{1}H-NMR and IR spectroscopies. The composition of the MPC unit was 30 mol%. The structural formula of PMB [12] is illustrated in Fig. 1. The PMB was resolved in ethanol, and the concentration was adjusted to 0.5% (wt/vol). The stainless steel specimens were immersed in the PMB solution and then dried on a clean bench. Before the specimens thus coated with PMB were used in culture experiments, they were immersed in calcium- and magnesium-free phosphate-buffered saline (PBS(–), pH 7.2)) for 30 min.

Bacterial preparation: *Staphylococcus aureus* (JCM 2151), *S. epidermidis* (JCM 2414), and *Pseudomonas aeruginosa* (JCM 2412) were purchased from Japan Collection of Microorganisms (Riken BioResource Center, Wako, Japan) and utilized in this investigation.

Cultivation experiments for confocal laser scanning microscope (CLSM) observation: Organisms were grown in the culture medium reported by Akiyama *et al.* [1], that was soybean-casein digest broth (Nihon Pharm., Tokyo, Japan) supplemented with the same amount of normal rabbit plasma (Denka Seiken, Tokyo, Japan). Cultivation experiments were performed following the previous reports [1, 9, 11, 27, 30]. Briefly, the specimen was placed on a 35-mm culture dish, and 2.0 m*l* of the culture medium containing bacteria was added. The concentration of bacteria was 3 × 10^8 cells/m*l*. The dish thus prepared was kept in an incubator at 37°C for 48 hr, and the observations of the specimens with a confocal scanning microscope were then performed.

Cultivation experiments for ATP assay: As was done in the cultivation experiments, the specimen was cultured in a 35-mm dish for 24 hr with the medium containing bacteria at a concentration 3 × 10^8 cells/m*l*. Subsequently, we took out the specimen from the dish and rinse away the medium with PBS(–). Then the specimen was transferred to another dish, and 2.0 m*l* of the culture medium supplemented with or without antibiotics was added. The antimicrobial agents were used to investigate the antibiotic resistance of the bacteria enveloped in the biofilm. The specimens were further incubated for another 24 hr in the incubator. The antibiotics utilized were either cefazolin sodium salt (100 μg/m*l*; Fujisawa, Osaka, Japan) or gentamicin sulfate (50 μg/m*l*; MP Biomedicals, Aurora, OH, U.S.A.). In the preparatory experiment, susceptibility of the bacteria to the antibiotics had been examined with the disk diffusion method [5]. We had observed a circular zone of inhibition surrounding a paper disk impregnated with gentamicin for all cases of *S. aureus*, *S. epidermidis*, and *P. aeruginosa*. On the other hand, a zone of inhibition surrounding cefazolin was resulted for *S. aureus* and *S. epidermidis* but not for *P. aeruginosa*. Hence the bacteria used in this experiment were susceptible to the utilized antibiotics, except the case of *P. aeruginosa* to cefazolin.

CLSM observations: The formation of biofilm was confirmed by the observation with a CLSM [1, 2, 4, 26, 30].

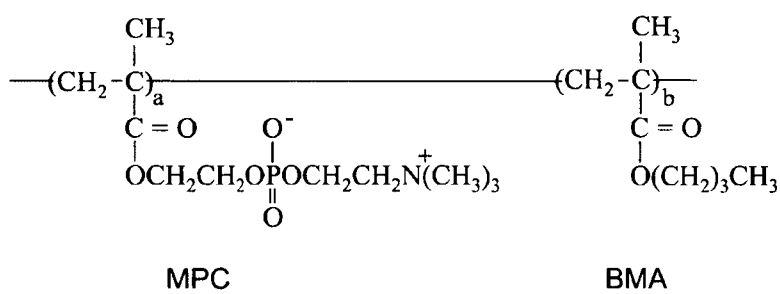

Fig. 1. Chemical formula of poly [MPC-co-n-butyl methacrylate (BMA)] (PMB) used in this study.

After cultivation with bacteria, the specimen was rinsed with PBS(–) and immersed into a 2.5% glutaraldehyde solution for 2 hr for fixation. The specimens were rinsed with PBS(–) again and immersed into an ethidium bromide solution (2 $\mu g/ml$; Molecular Probes, Carlsbad, CA, U.S.A.) for 5 min for the staining of bacterial nucleic acid in biofilms [26]; they were then immersed into a fluorescein isothiocyanate (FITC)-conjugated concanavalin A solution (50 $\mu g/ml$; Sigma-Aldrich, St. Louis, MO, U.S.A.) for 3 min for the staining of polysaccharides in biofilms [1, 30]. A CLSM (LSM 5 PASCAL; Carl Zeiss MicroImaging GmbH, Jena, Germany) was used for fluorescent observation. The observation was carried out for 10 specimens.

Measurement of the number of bacteria by ATP assay: An ATP-dependent luminescence reaction between luciferin and luciferase was utilized to count the number of bacteria [20, 21]. After incubation, the specimen was rinsed with PBS(–). Subsequently, ATP in the bacterial cytoplasm was extracted by sonication for 10 min from the specimen immersed in 0.5 m*l* of 0.5% trichloroacetic acid solution. The amount of ATP was measured using an ATP assay kit (ENLITEN ATP Assay System Bioluminescence Detection Kit; Promega, Madison, WI, U.S.A.) and a luminometer (Auto Lumat; EG&G Berthold, Bad Wildbad, Germany). The relations between the number of bacteria measured by a hemocytometer for bacterial counting (A161; SLGC, Tokyo, Japan) and the relative light unit (RLU) measured by the ATP assay system were established for the respective bacteria. Utilizing these standard relations, the RLU values measured in the experiments were converted to the numbers of bacteria. The measurements were carried out for 10 specimens.

Statistical analysis: The obtained data were analyzed by two-way ANOVA to determine the effectiveness of PMB coating and antibiotics in decreasing the number of bacteria. Subsequently, statistical differences among cases in the noncoated and PMB-coated surfaces were examined by Scheffe's multiple comparison test.

RESULTS

CLSM observation: Figure 2 shows the example of a typical observation by CLSM. In every case of exposure to *S. aureus*, *S. epidermidis*, and *P. aeruginosa*, many bacteria and polysaccharides were revealed to exist on the noncoated surfaces of the specimens, as shown in Figs. 2(a), 2(c), and 2(e). On the other hand, there was little or no trace of bacteria or polysaccharides on MPC-coated surfaces, as shown in Figs. 2(b), 2(d), and 2(f). Accordingly, we concluded that biofilm was formed on the noncoated surfaces whereas no biofilm was formed on MPC-coated surfaces.

Number of bacteria measured by ATP assay: The ATP assay was performed to measure the number of bacteria and the data are presented in Table 1. Furthermore, statistical analysis was carried out and significant differences between the experimental groups were examined. The analyzed results are illustrated in Fig. 3. In the cases of *S. aureus* and *S. epidermidis*, application of either kind of antibiotics decreased the number of bacteria on the noncoated surfaces ($p<0.01$). On the PMB-coated surfaces, their numbers were smaller than those on the noncoated surfaces ($p<0.01$). The application of antibiotics further decreased the number ($p<0.01$). In the cases of *P. aeruginosa*, application of gentamicin decreased the number ($p<0.01$) whereas cefazolin increased the number of bacteria ($p<0.01$) on the noncoated surfaces. On the PMB-coated surfaces, their numbers were smaller than those on the noncoated surfaces ($p<0.01$). The application of gentamicin decreased the number ($p<0.01$) whereas cefazolin increased the number ($p<0.01$).

DISCUSSION

Device-associated infections are caused by the bacteria adhered to internal prosthetic devices and are thought to occur through many critical steps [3, 7, 10, 18, 22]. These steps are as follows: adsorbance of various molecules, including peptides and proteins, onto the surfaces of the devices; the mediation of bacterial attachment via these molecules; and the formation of biofilms. If biofilm formation is completed, the bacteria in the biofilm are protected from the biological defense mechanism, and furthermore, from the administered antibacterial agents. Hence, the formation of biofilms on the surface of devices establishes a refractory infection, i.e., device-associated infections [6, 8, 19, 24, 27, 28].

The MPC polymer has the phospholipid polar group and the methacryloyl group in its molecular structure. This confers MPC excellent polymerization ability. The MPC polymers have desirable properties for the inhibition of protein adsorption and cell adhesion. Recently, the MPC polymer was utilized for the coating of medical devices such as artificial blood vessels, implantable artificial hearts, and artificial lungs and successful preventions of thrombus formation were reported [13–17, 25]. Since the attachment of bacteria to the material's surface is also mediated by adsorbed proteins, MPC might be most favorably utilized to inhibit the formation of biofilms. In this investigation, we utilized the PMB as an MPC polymer for the coating materials of metallic specimens to explore the possible uses for the prevention of device-associated infections.

S. aureus, *S. epidermidis*, and *P. aeruginosa* were chosen for this experiment since these bacteria are the most common species causing device-associated infections in the field of orthopedics, and they are also implicated in the pathogenesis of osteomyelitis [10]. Their cultivation was performed following the biofilm formation assay established in previous reports [1, 9, 27, 30]. Then the specimens were stained with ethidium bromide for bacterial nucleic acid and (FITC)-conjugated concanavalin A for polysaccharides and examined by a CLSM, which was also adopted in the biofilm formation assay [1, 26, 30].

In the experiments, the observations by a CLSM clearly demonstrated the presence of bacteria and the existence of polysaccharides on the noncoated surfaces of specimens, as

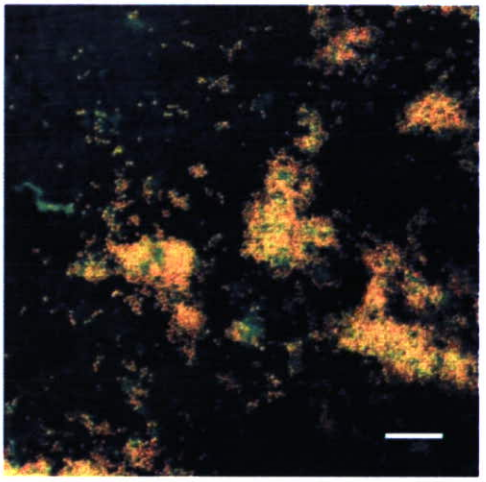

(a) *S. aureus* on noncoated surface

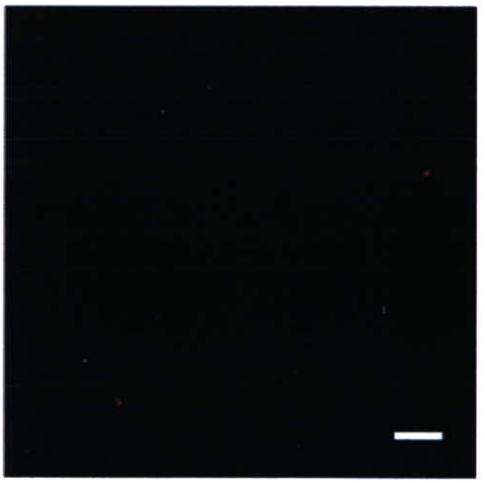

(b) *S. aureus* on PBM-coated surface

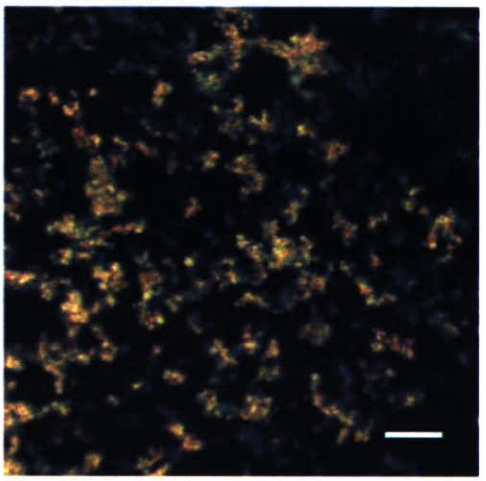

(c) *S. epidermidis* on noncoated surface

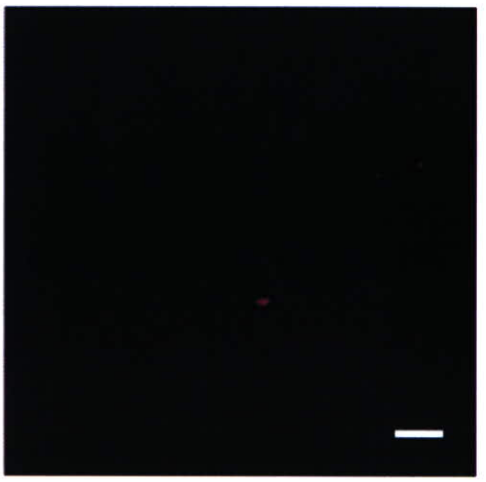

(d) *S. epidermidis* on PMB-coated surface

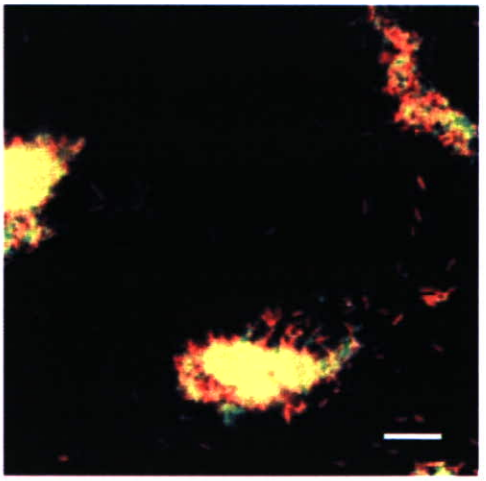

(e) *P. aeruginosa* on noncoated surface

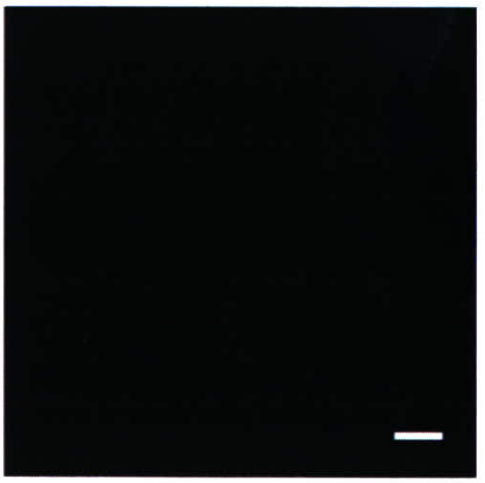

(f) *P. aeruginosa* on PMB-coated surface

Table 1. Number of bacteria (10^5 cells/specimen) on noncoated and PMB-coated surfaces on specimens after 24 hr incubation in which antibiotics were absent or either cefazolin or gentamicin were added, following 24 hr incubation without antibiotics. The values are represented as mean ± SD

coating		none			PMB coating	
antibiotics	none	cefazolin	gentamicin	none	cefazolin	gentamicin
S. aureus	2702 ± 303	1722 ± 200	1621 ± 91	163.3 ± 9.6	1.469 ± 0.305	1.263 ± 0.134
S. epidermidis	41.99 ± 6.27	1.677 ± 0.186	1.789 ± 0.249	0.8291 ± 0.1099	0.4283 ± 0.0486	0.3172 ± 0.0357
P. aeruginoza	2008 ± 263	6080 ± 385	1278 ± 295	29.74 ± 2.12	48.92 ± 2.37	9.209 ± 0.345

shown in Figs. 2(a), 2(c), and 2(e), which provided a morphological evidence of the formation of biofilms.

The number of bacteria was measured by the ATP assay, and it was demonstrated that the number of bacteria on the noncoated surface of the specimens decreased with statistical significance following the application of cefazolin or gentamicin in the cases of *S. aureus*, as shown in Fig. 3(a). However, the application of antibiotics did not even halve the number of bacteria. The number of *P. aeruginosa* was not halved by the antibiotics in a similar manner as shown in Fig. 3(c). Contrastively, the number of bacterial was increased when they were cultivated in the cefazolin added medium. This might be attributed to that the specimens were incubated for 24 hr in medium without antibiotics and then they were incubated for another 24 hr in new medium containing cefazolin, to which *P. aeruginosa* was not susceptible. In either case of bacteria, anyhow, the fact that antibiotics could not halve the bacteria provided a functional evidence of the formation of biofilms, in which the bacteria were enveloped and protected from the antibiotics. On the other hand, the number of *S. epidermidis* bacteria on the noncoated surface was decreased to less than 1/10 times of the original number by the application of the antibiotics, as shown in Fig. 3(b). The biofilms formed by *S. epidermidis* were seemingly less effective in protecting the bacteria.

In contrast, on the PMB-coated surfaces, the bacteria and polysaccharides were not detected by confocal laser microscopy, as shown in Figs. 2(b), 2(d), and 2(f); this provided a morphological evidence of the absence of biofilms.

The ATP assay demonstrated that the number of bacteria on the PMB-coated surfaces of the specimens decreased with statistical significance compared to those on noncoated surfaces. Although the number of bacteria decreased approximately only 1/20 times the original number in the cases of *S. aureus*, the application of antibiotics further decreased the number of bacteria to approximately 1/2000 times, as shown in Fig. 3(a). This phenomenon proved that the bacteria are not protected from antibiotics and implies that *S. aureus* on the PMB-coated surface, which could not be removed by rinsing, did not form a biofilm. Similarly, the number of *S. epidermidis* was decreased to approximately 1/50 times the original number on the PMB-coated surface, and the application of antibiotics further decreased the number to approximately 1/1200 times, as shown in Fig. 3(b). The number of *P. aeruginosa* was decreased to approximately 1/70 times on a PMB-coated surface, and the application of gentamicin further decreased the number to approximately 1/220 times, but cefazolin was not effective in reducing the number of bacteria, as shown in Fig. 3(c). The difference in the response toward cefazolin and gentamicin is explained by the fact that cefazolin is a beta-lactam antibiotic, which is active against gram-positive bacteria such as *Staphylococcus* sp. but not against *P. aeruginosa*, and gentamicin is an amino-glycoside antibiotic that is active against gram-negative bacteria, including *P. aeruginosa* as well as gram-negative bacteria.

Hence, the observed decreases in the number of bacteria by the application of antibiotics provided a functional evidence that PMB coating prevented the formation of biofilms.

Thus, we concluded that the PMB coating effectively prevented the formation of bacterial biofilms on the surface of metallic specimens. Although our results were limited to *in vitro* experiments and further investigations are necessary, the decrease in the number of bacteria in the order of 1/100 to 1/1,000 is encouraging. We expect that the PMB coating combined with validated uses of antibiotics might provide an effective approach to the simultaneous achievement of a biocompatible surface of devices and the prevention of the device-associated infections.

Further investigations are necessary to achieve successful clinical applications. One of the issues to be examined is, durability of the coating. Yoneyama [32] implanted the MPC polymer coated artificial vessels made of polyester fibers to carotid arteries of rabbit, and observed the antithrombogenicity as long as 4 weeks after implantation. We confirmed the prevention of biofilm forming with the use of PMB coating in 48 hr experiments; however, verification of the durability should be performed. Furthremore, the toxicity of the polymer eluted from the coating layer should be examined.

Fig. 2. CLSM observations of the specimens with noncoated and PMB-coated surfaces after 48 hr incubation. (a). *S. aureus* on noncoated surface, (b) *S. aureus* on PMB-coated surface, (c) *S. epidermidis* on noncoated surface, (d) *S. epidermidis* on PMB-coated surface, (e) *P. aeruginosa* on noncoated surface, (f) *P. aeruginosa* on PMB-coated surface. The nucleic acid in bacteria was stained with ethidium bromide (red) and polysaccharide by FITC conjugated concanavalin A (green). Bar is 10 μm. Many bacteria and polysaccharides were detected on the noncoated surfaces, whereas they were very few on PMB-coated surfaces.

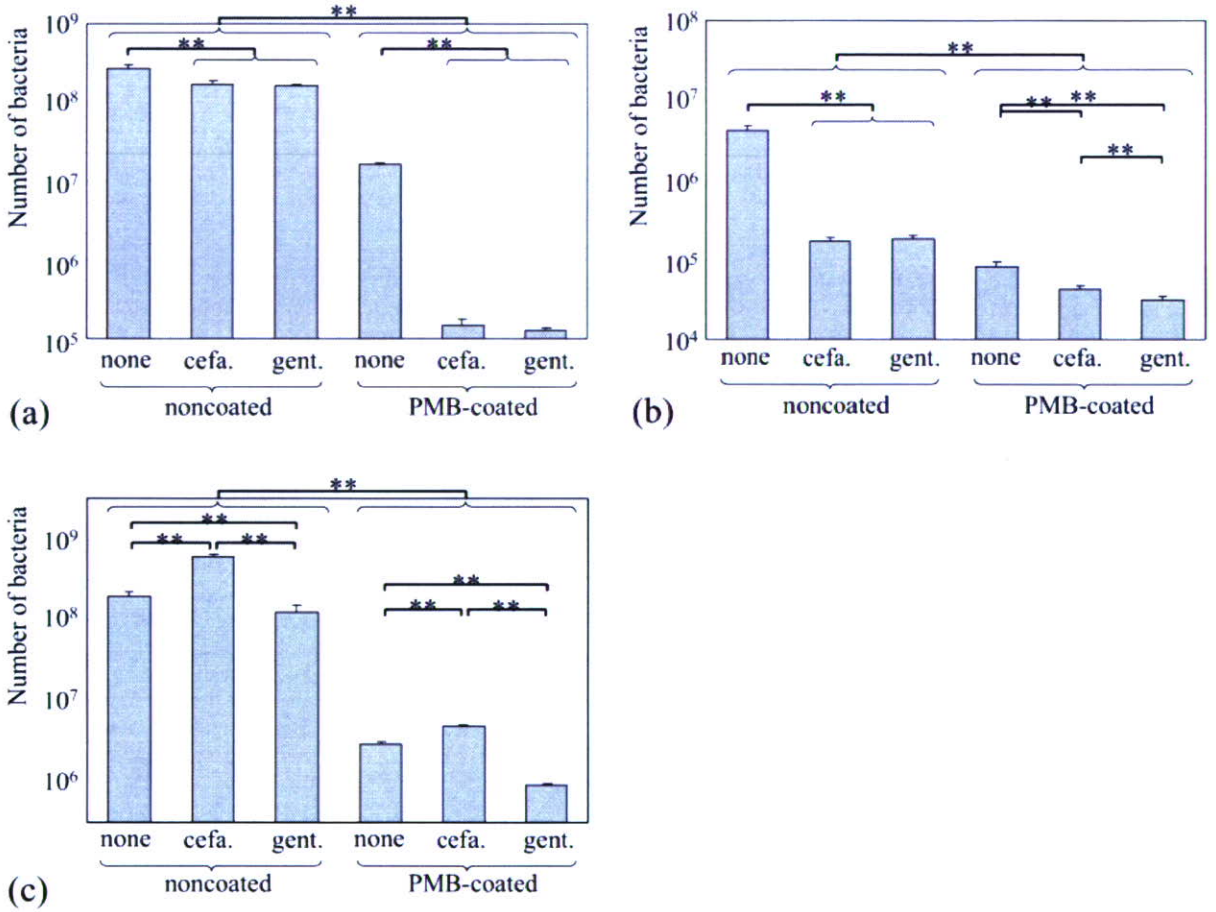

Fig. 3. Number of bacteria on noncoated and PMB-coated surfaces of specimens after 24 hr incubation in which antibiotics were absent or either cefazolin or gentamicin were added, following 24 hr incubation without antibiotics. (a) *S. aureus*, (b) *S. epidermidis*, (c) *P. aeruginosa*.

(a) Number of *S. aureus* on the surfaces on specimens. ** Significant difference ($p<0.01$) was observed; between noncoated and PMB-coated surfaces; between cases in which antibiotics were either absent or present on the noncoated and PMB-coated surfaces.

(b) Number of *S. epidermidis* on the surfaces on specimens. ** Significant difference ($p<0.01$) was observed; between noncoated and PMB-coated surfaces; between cases in which antibiotics were absent and cefazolin and gentamicin were added on the PMB-coated surfaces.

(c) Number of *P. aeruginosa* on the surfaces on specimens. ** Significant difference ($p<0.01$) was observed; between noncoated and PMB-coated surfaces; between cases in which antibiotics were absent, cefazolin and gentamicin were added on the noncoated and PMB-coated surfaces.

ACKNOWLEDGEMENT. This study was partially supported by Grants-in-Aid for Scientific Research on Priority Area (No.15086206) from the Ministry of Education, Culture, Sports, Science and Technology of Japan.

REFERENCES

1. Akiyama, H., Huh, W. K. and Fujii, K. 2002. Confocal laser microscopic observation of glycocalyx production by *Staphylococcus* aureus *in vitro*. *J. Dermatol. Sci.* **29**: 54–61.
2. Caldwell, D. E., Korber, D. R. and Lawrence, J. R. 1992. Confocal laser microscopy and digital image analysis. *Adv. Microb. Ecol.* **12**: 1–67.
3. Chang, C. C. and Merritt, K. 1994. Infection at the site of implanted materials with and without preadhered bacteria. *J. Orthop. Res.* **12**: 526–531.
4. Costerton, J. W., Lewandowski, Z., Caldwell, D. E., Korber, D. R. and Lappin-Scott, H. M. 1995. Microbial biofilms. *Annu. Rev. Microbiol.* **49**: 711–745.
5. Felten, A., Grandry, B., Lagrange, P. H. and Casin, I. 2002. Evaluation of three techniques for detection of low-level methicillin-resistant *Staphylococcus aureus* (MRSA): a disk diffusion method with cefoxitin and moxalactam, the Vitek 2 System, and the MRSA-Screen Latex Agglutination Test. *J. Clin. Micorbiol.* **40**: 2766–2771.
6. Gristina, A. G. 1987. Biomaterial centered infection. Microbial adhesion versus tissue integration. *Science* **27**: 1588–1595.
7. Harris, L. G., Foster, S. J. and Richards, R. G. 2002. An introduction to *Staphylococcus aureus*, and techniques for identify-

ing and quantifying *S. aureus* adhesions in relation to adhesion to biomaterials: review. *Eur. Cell Mater.* **4**: 39–60.
8. Harris, L. G., Tosatti, S. and Wieland, M. 2004. *Staphylococcus aureus* adhesion to titanium oxide surfaces coated with non-functionized poly(L-lysine)-grafted- poly(ethylene glycol) copolymers. *Biomaterials* **25**: 4135–4148.
9. Hirota, K., Murakami, K. and Nemoto, K. 2005. Coating of a surface with 2-methacryloyloxyethyl phosphorylcholine (MPC) co-polymer significantly reduces retention of human pathogenic microorganisms. *FEMS Microbiol. Lett.* **248**: 37–45.
10. Hudson, M. C., Ramp, W. K. and Frankenburg, K. P. 1999. *Staphylococcus aureus* adhesion to bone matrix and bone-associated biomaterials. *FEMS Microbiol. Lett.* **173**: 279–284.
11. Hussain, M., Hasting, J. G. and White, P. J. 1991. Isolation and composition of the extracellular slime made by coagulase-negative staphylococci in a chemically defined medium. *J. Infect. Dis.* **163**: 534–541.
12. Ishihara, K., Fukumoto, K., Iwasaki, Y. and Nakabayashi, N. 1999. Modification of polysulfone with phospholipid polymer for improvement of the blood compatibility. Part 1. Surface characterization. *Biomaterials* **20**: 1545–1551.
13. Ishihara, K., Oshida, H. and Endo, Y. 1992. Hemocompatibility of human whole blood on polymers with a phospholipid polar group and its mechanism. *J. Biomed. Mater. Res.* **26**: 1543–1552.
14. Ishihara, K., Ueda, T. and Nakabayashi, N. 1990. Preparation of phospholipid polymers and their properties as polymer hydrogel membranes. *Polym. J.* **22**: 355–360.
15. Ishihara, K., Ziats, N. P. and Tierney, B. P. 1991. Protein adsorption from human plasma is reduced on phospholipid polymers. *J. Biomed. Mater. Res.* **25**: 1397–1407.
16. Iwasaki, Y. and Ishihara, K. 2005. Phosphorylcholine-containing polymers for biomedical applications. *Anal. Bioanal. Chem.* **381**: 534–546.
17. Iwasaki, Y., Nakabayashi, N. and Ishihara, K. 2003. *In vitro* and *ex vivo* blood compatibility study of 2-methacryloyloxyethyl phosphorylcholine (MPC) copolymer-coated hemodialysis hollow fibers. *J. Artif. Organs* **6**: 260–266.
18. Jeanine, A., Jaques, O. G. and Anne, M. 1999. Tracking adhesion factors in *Staphylococcus caprae* strains responsible for human bone infections following implantation of orthopaedic material. *Microbiology* **145**: 2033–2042.
19. Jennings, D. A., Morykwas, M. J., Burns, W. W., Crook M. E., Hudson, W. P. and Argenta, L. C. 1991. *In vitro* adhesion of endogenous skin microorganism to breast prostheses. *Ann. Plast. Surg.* **27**: 216–220.
20. Lundin, A. and Thore, A. 1975. Analytical information obtainable by evaluation of the time course of firefly bioluminescence in the assay of ATP. *Anal. Biochem.* **66**: 47–63.
21. McElroy, W. D. and DeLuca, M. A. 1983. Firefly and bacterial luminescence. Basic science and applications. *J. Appl. Biochem.* **5**: 197–209.
22. Merritt, K. and Chang, C. C. 1991. Factors influencing bacterial adherence to biomaterials. *J. Biomater. Appl.* **5**: 185–203.
23. Merritt, K. and Dowd, J. D. 1987. Role of internal fixation in infection of open fracture: Studies with *Staphylococcus aureus* and *Proteus mirabilis*. *J. Orthop. Res.* **5**: 23–28.
24. Montanaro, L., Arciola, C. R. and Baldassarri, L. 1999. Presence and expression of collagen adhesion gene (can) and slime production in *Staphylpcoccus aureus* strains from orthopaedic prosthesis infection. *Biomaterials* **20**: 1945–1949.
25. Ogawa, R., Watanabe, J. and Ishihara, K. 2003. Domain-controlled polymer alloy composed of segmented polyurethane and phospholipid polymer for biomedical applications. *Sci. Technol. Adv. Mater.* **4**: 523–530.
26. Qian, Z., Stoodley, P. and Pitt, W. G. 1996. Effect of low-intensity ultrasound upon biofilm structure from confocal scanning laser microscopy observation. *Biomaterials* **17**: 1975–1980.
27. Ramage, G., Tunney, M. M. and Patrick, S. 2003. Formation of propinibacterium acnes biofilms on orthopaedic biomaterials and their susceptibility to antimicrobials. *Biomaterials* **24**: 3221–3227.
28. Sheehan, E., McKenna, J. and Mulhall, K. J. 2004. Adhesion of *Staphylococcus* to orthopaedic materials, an *in vivo* study. *J. Orthop. Res.* **22**: 39–43.
29. Takahashi, H. 2001. Examination about the bio-film formation prevention effect of the antibacterial new coating catheter material which blended citrate silver and lecithin. *Kansenshoushi* **75**: 678–685 (in Japanese).
30. Takenaka, S., Iwaku, M. and Hoshino, E. 2001. Artificial *Pseudomonas aeruginosa* biofilm and confocal laser scanning microscopic analysis. *J. Infect. Chemother.* **7**: 87–93.
31. Wassall, M. A., Santin, M. and Isalberti, C. 1997. Adhesion of bacterial to stainless steel and silver-coated orthopedic external fixation pins. *J. Biomed. Mater. Res.* **36**: 325–330.
32. Yoneyama, T., Ito, M., Sugihara, K., Ishihara, K. and Nakabayashi, N. 2000. Small diameter vascular prosthesis with a non-thrombogenic phospholipid polymer surface: preliminary study of a new concept for functioning in the absence of pseudo- or neointima formation. *Artif. Organs* **24**: 23–28.

J Mater Sci: Mater Med (2008) 19:1009–1016
DOI 10.1007/s10856-007-3076-8

Mechanical, setting, and biological properties of bone cements containing micron-sized titania particles

Koji Goto · Masami Hashimoto · Hiroaki Takadama · Jiro Tamura · Shunsuke Fujibayashi · Keiichi Kawanabe · Tadashi Kokubo · Takashi Nakamura

Received: 18 January 2007 / Accepted: 3 April 2007 / Published online: 1 August 2007

Abstract In this study, polymethylmethacrylate-based composite cements containing 40–55.6 wt% micron-sized titania (titanium oxide) particles were developed, and their mechanical, setting, and biological properties evaluated. Three types of composite cement containing 40, 50, and 55.6 wt% silanized titania were designated ST2-40c, ST2-50c, and ST2-56c, respectively. In animal experiments, ST2-50c and ST2-56c were implanted into rat tibiae and solidified in situ. An affinity index was used to evaluate osteoconductivity. Compressive and bending strength of ST2-56c was 147.7 ± 3.2 and 69.3 ± 7.4; those of the other cements exceeded 100 MPa and 50 MPa, respectively. The affinity indices of ST2-56c were 42.1 ± 12.9 at six weeks and 53.4 ± 16.6 at 12 weeks, and were significantly higher than for ST2-50c and a commercial PMMA bone cement within 12 weeks. Our data indicate that bone cement containing micron-sized titania particles can be applied to prosthesis fixation as well as vertebroplasty, and ST2-56c is a good candidate cement.

K. Goto (✉) · J. Tamura · S. Fujibayashi · K. Kawanabe · T. Nakamura
Department of Orthopaedic Surgery, Faculty of Medicine, Kyoto University, Kawahara-cho 54, Shogoin, Sakyo-ku, Kyoto 606-8507, Japan
e-mail: k.g.bau@kuhp.kyoto-u.ac.jp

M. Hashimoto · H. Takadama
Japan Fine Ceramics Center, Mutsuno 2-4-1, Atsuta-ku, Nagoya 456-8587, Japan

T. Kokubo
Research Institute for Science and Technology, Chubu University, 1200 Matsumoto-cho, Kasugai 487-8501, Japan

Introduction

Since the 1990s, many types of bioactive bone cement have been developed to overcome the disadvantages of polymethylmethacrylate (PMMA) bone cement [1], especially its lack of bone-bonding ability, which occasionally leads to aseptic loosening of prostheses used for arthroplasty [2, 3]. However, the acceptable long-term clinical results of PMMA bone cement [4, 5], and concerns about the long-term stability of bioactive fillers in the cements have so far prevented bioactive bone cements being used for the fixation of prostheses in arthroplasty. Recently, anatase and rutile, crystal phases of titania, have been shown to have excellent in vitro apatite-forming ability and in vivo bioactivity [6–9]. Titania is stable in the body and does not degrade, so that bone cements containing bioactive titania filler can be stable in the body environment. Then a composite bone cement containing nanosized anatase-type titania particles was developed, and it was reported that certain compositions of the cement had good osteoconductivity [10]. However, some of the nanosized titania particles tended to aggregate in the cement. As a result, the cements containing nanosized titania particles did not reach the minimum bending strength required by the ISO 5833 standard (50 MPa), which is applied to acrylic resin cements used for prosthesis fixation, and could be applied clinically for vertebroplasty, but not for prosthesis fixation. One possible resolution of this problem was to increase the titania particle size. In this study, composite cements that contained micron-sized titania particles were developed. Preliminary PMMA cement candidates with different amounts of titania particles were examined for their mechanical properties and apatite forming ability in vitro [11], and two promising composites were used in an implantation study.

The purpose of the study was to evaluate the mechanical and setting properties, and osteoconductivity of cements containing micron-sized titania.

Materials and methods

Preparation of powders

Titania powder

Plate-like titania powder (Ishihara Sangyo Kaisha, Osaka, Japan) with an average particle size of 1.55 μm was used as supplied. The particle size distribution of the titania powder, which was determined using a laser diffraction analyzer (LA-910; Horiba, Kyoto, Japan), is shown in Fig. 1a. Powder X-ray diffraction of the particles revealed that the titania particles were composed of anatase and rutile phases (Fig. 1b). The weight ratio of anatase:rutile in the 1.55 μm titania powder was about one, based on the peak intensities of each diffraction pattern. The titania powder was mixed into three types of TiO_2-dispersed cements with 40, 50, and 55.6 wt% TiO_2, designated ST2-40c, ST2-50c, and ST2-56c, respectively.

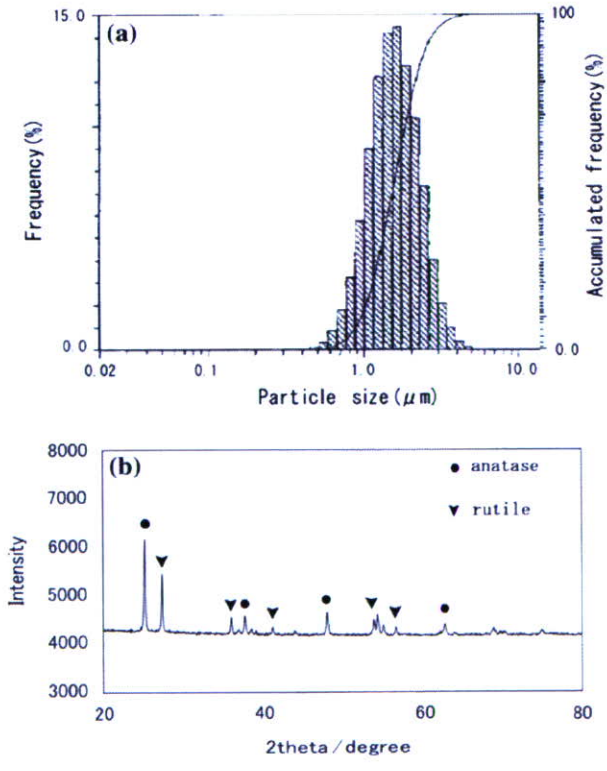

Fig. 1 (**a**) Titania powder particle size distribution. (**b**) Powder X-ray diffraction data for titania powder

Titania powders were treated with a silane-coupling agent as follows: 1.1 g of 3-methacryloxypropyltrimethoxysilane (Shin-Etsu Chemical Co., Tokyo), 1.6 g of ethanol and 0.2 g of deionized water were mixed on a magnetic stirrer for 10 min. The solution containing the silane-coupling agent was added to 110 g of the TiO_2 powder and mixed in a shaker mixer (TURBULA T2F, W. A. Bachofen AG Co., Basel, Switzerland) at 25 °C for 1 h. The rotation speed was 96 rpm. After mixing, the mixtures were dried and heated at 130 °C for 5 min.

Polymethylmethacrylate powder

Spherical PMMA powder, synthesized by suspension polymerization [12], with an average molecular weight of 270,000 Da and an average particle size of 5 μm (standard deviation: 2 μm) [13] was used.

Preparation of the liquid

Liquid methacrylate (MMA) monomer (Wako Pure Chemical Industries, Osaka, Japan) was used.

Cement preparation

Four types of cement, designated ST2-40c, ST2-50c, ST2-56c, and PMMAc, were prepared. PMMAc was a commercially available PMMA-based bone cement (Osteobond; Zimmer, Warsaw, IN, USA) and was used as a control material. The composition of each TiO_2-containing cement is shown in Table 1. As an initiator, benzoyl peroxide (Nacalai Tesque, Kyoto, Japan) was added to the powder at 4.0 wt% of the monomer, and as an accelerator, *N,N*-dimethyl-*p*-toluidine (Kanto Chemical Co. Inc., Tokyo, Japan) was dissolved in the liquid to 2.0 wt% of the monomer. Each cement was prepared by mixing the powder with the liquid for 1 min.

Mechanical testing

The compressive strength, bending strength, and bending modulus of ST2-40c, ST2-50c, and ST2-56c were mea-

Table 1 Composition of PMMA-based cements containing titania powders

Cement	Powders[a] (wt%)		Liquid[b] (wt%) MMA
	Titania	PMMA	
ST2-40c	40	20	40
ST2-50c	50	16.7	33.3
ST2-56c	55.6	14.6	29.6

[a] Benzoyl peroxide was added at 4 wt% of the MMA

[b] *N,N*-Dimethyl-*p*-toluidine was added at 2 wt% of the MMA

sured using five prehardened cement specimens for each mechanical test. For mechanical bending analysis, four-point bending testing was performed with rectangular specimens sized to 70 mm × 20 mm × 5 mm. For compressive mechanical analysis, prehardened cylindrical cement specimens, 6 mm in diameter and 12 mm in length, were prepared. The tests were carried out according to ISO 5833, with a Model 5582 testing machine (Instron Corporation, Canton, MA, USA); the test conditions were previously described in detail [10].

Some of the bending specimens were prepared for observation with a scanning electron microscope (SEM, S-4700; Hitachi, Tokyo, Japan), and the fracture surfaces were analyzed to determine the microstructure of the cements.

Setting of the cements

The cement pastes were mixed for 1 min and cast in a cylindrical mold made of polytetrafluoroethylene (inner diameter 60 mm, inner depth 20 mm). The temperature change during the setting reaction was measured using an infrared thermometer under ambient conditions of 23 °C and 54–65% humidity. By plotting the time and temperature, the setting time of each cement was determined according to ISO 5833.

Animal experiments

Eight-week-old male Wistar rats weighing 180–230 g were used for the implantation study. The animals were reared and the experiments carried out at the Institute of Laboratory Animals, Faculty of Medicine, Kyoto University, under the institutional guidelines for use of experimental animals set by Kyoto University.

The rats were operated on under general anesthesia induced by intraperitoneal injection of sodium 5-ethyl-5-(1-methylbutyl) barbiturate (Nembutal [pentobarbital]; Dainippon Pharmaceutical Company, Osaka, Japan) at 40 mg/kg of body weight. Cortical bone defects measuring 2 mm × 7 mm were created in the medial aspect of the proximal metaphyses of both tibiae, and the bone marrow was curetted. The intramedullary canals of both bone defects were irrigated with physiological saline, and paste-form cement was inserted manually and allowed to cure in situ for evaluation of osteoconductivity [10, 14, 15]. Twelve rats (24 legs) were used for the evaluation of osteoconductivity, with ST2-50c and ST2-56c each being used in 12 legs. Half the rats in each subgroup were killed at six and 12 weeks after the operation.

To confirm the high radiopacity of ST2-56c, another operation was performed using an additional rat. After a hole had been made in the intercondylar space of the distal femur, and the intramedullary canal of the total femur was curetted and irrigated with physiological saline, ST2-56c and PMMAc in liquid phase were inserted into each of the bilateral canals using a syringe fitted with an 18-gauge needle, and this was allowed to cure in situ. One day after the operation, the rat was killed and an X-ray radiograph of the femurs was taken.

Micrographic examination

Specimens were dehydrated through a graded series of ethanol (70, 80, 90, 99, and 100 vol%) and embedded in epoxy resin (Epofix, Struers Co., Copenhagen, Denmark). Thin sections (100 or 500 μm thick) were cut with a band saw (BS-3000; Exakt, Norderstedt, Germany) perpendicular to the axis of the tibias containing the cement. Four sections could be typically made from each leg. The third section (100 μm thick) from the most distal portion of each leg was ground to a thickness of 60–80 μm using a grinding–sliding machine (Microgrinding MG-4000; Exakt) for Giemsa surface staining. The second section (100 μm thick) from each leg was prepared for contact microradiography. The first and fourth sections (500 μm thick) from each leg were polished with diamond paper and coated with a thin layer of carbon for observation by SEM (S-4700, Hitachi, Tokyo, Japan). Some of those specimens were analyzed using an energy-dispersive X-ray microanalyzer (EMAX-7000; Horiba, Kyoto, Japan) attached to the SEM (SEM–EDX). To evaluate osteoconductivity, affinity indices (%) for each subgroup were calculated as previously described [10, 14, 15].

Statistical analysis

Values were expressed as means and standard deviations (SD). Values of mechanical properties for each cement and the affinity indices for each cement at each time interval were compared using one-way analysis of variance. Subsequently, possible differences were investigated using Fisher's PLSD post hoc statistical test using StatView (version 5.0) for Windows. A P value less than 0.01 was considered statistically significant.

Results

Mechanical properties

The results of the mechanical property measurement and their statistical analyses are shown in Table 2. The ultimate compressive strength, flexural strength, and flexural modulus increased as the titania content of the cement increased. SEM revealed that titania particles were

Table 2 Mechanical properties of ST2-40c, ST2-50c, ST2-56c, and PMMAc (means ± SD, n = 5)

	Compressive strength (MPa)	Bending strength (MPa)	Bending modulus (GPa)
ST2-40c	106.1 ± 5.5*	54.3 ± 6.6	3.10 ± 0.47
ST2-50c	127.9 ± 6.4*	57.8 ± 4.1	3.88 ± 0.46
ST2-56c	147.7 ± 3.2*	69.3 ± 7.4**	4.07 ± 0.83
PMMAc	87.9 ± 2.7*	59.4 ± 7.8	1.56 ± 0.28***

The values for PMMAc were derived from our previous study[10]

* All pairs were significantly different

** Significantly different to ST2-40c

*** Significantly different to all the other cements

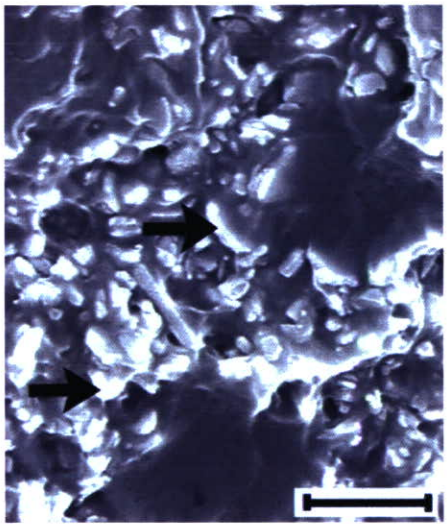

Fig. 2 Scanning electron micrograph of the fracture surface of ST2-56c. Arrows indicate titania particles. Bar = 3 μm

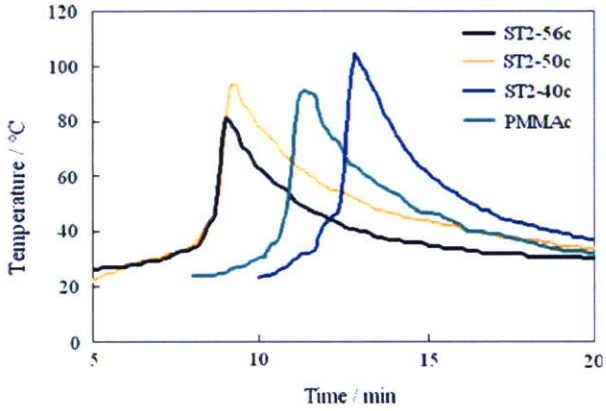

Fig. 3 Heat evolution curves for the setting reactions of ST2-50c, ST2-56c, PMMAc, and ST2-40c

uniformly dispersed and interacted well with the PMMA, and aggregates of titania particles could not be seen in the fracture surfaces of each cement (Fig. 2).

Setting time and peak temperature

The results of the temperature plotting of the cements are shown in Fig. 3. The setting times were 12 min 40 s for ST2-40c, 9 min 0 s for ST2-50c, 8 min 50 s for ST2-56c, and 11 min 0 s for PMMAc. The peak temperatures were 104 °C for ST2-40c, 93 °C for ST2-50c, 81 °C for ST2-56c, and 91 °C for PMMAc. The setting time of the cements containing titania particles reduced and the peak temperature decreased as the titania filler content increased.

Radiopacity

The ST2-56c in the femur was much more radiopaque than the PMMAc (Fig. 4). Both the ST2-56c and PMMAc were injected through an 18-gauge needle without problems, although ST2-56c was more easily injected.

Evaluation of the bone–cement interface

Giemsa surface staining indicated that there was typically no inflammatory reaction around ST2-50c and ST2-56c (Fig. 5a, b). The intervening soft tissue layer between cement and bone was more often seen around ST2-50c than ST2-56c at each time interval. For ST2-56c, no significant change in appearance could be seen with Giemsa surface staining between the 6- and 12-week specimens. On the other hand, for ST2-50c, there appeared to be less intervening soft tissue layer between the cement and bone in the 12-week specimens than in the 6-week specimens.

Low magnification SEM revealed that ST2-56c was in direct contact with bone over large areas within six weeks, whereas ST2-50c was in contact with bone in only small areas (Fig. 6a, b). In the 12-week specimens, both ST2-56c and ST2-50c were in direct contact with bone over large areas (Fig. 6c, d). Both ST2-50c and ST2-56c showed a marginal white line 30–60 μm wide at each time interval,

Fig. 4 X-ray radiograph of bilateral femurs of a rat one day after the operation

regardless of whether they were in contact with bone. These findings were also revealed by contact microradiography, in which each cement appeared to be in direct contact with bone over larger areas than in the SEM observation (Fig. 7a, b).

Backscattered SEM at high magnification revealed that both ST2-56c and ST2-50c were in direct contact with bone within six weeks, but a thin intervening soft tissue layer less than 10 μm thick was often observed between ST2-50c and the bone (Fig. 8a, b). It also showed that ST2-50c and ST2-56c were in contact with bone via a white line, which was demonstrated by SEM–EDX analyses to be a Ti-rich layer (Fig. 8c). An increase in the intensity of calcium was also detected along the outer margin of this white line (Fig. 8c).

Evaluation of osteoconductivity

The affinity indices for all of the cements at six and 12 weeks, and the statistical comparisons, are shown in Fig. 9.

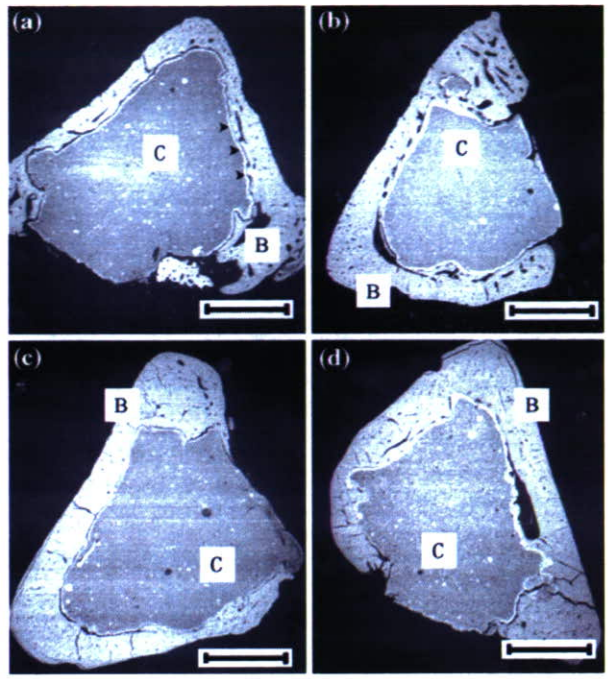

Fig. 6 Low magnification scanning electron micrographs of (**a**) ST2-50c and (**b**) ST2-56c in rat tibiae six weeks after implantation; (**c**) ST2-50c and (**d**) ST2-56c in rat tibiae 12 weeks after implantation. C, cement; B, bone; Arrowheads indicate the white line. Bar = 30 μm

Discussion

In preliminarily trials, it was attempted to prepare cements containing over 60 wt% micron-sized titania particles, but it was often difficult to effectively mix the powder and the liquid. Preliminary in vitro studies revealed that the apatite-forming ability of the composite cements increased with the content of titania particles. Because ST2-50c and ST2-56c were consistently made in a well-mixed form and were expected to have better osteoconductivity than ST2-40c, as judged from the in vitro studies, they were chosen for the animal study.

With the previously reported composite bone cement containing nanosized anatase-type titania particles, it was difficult to disperse the titania particles uniformly in the

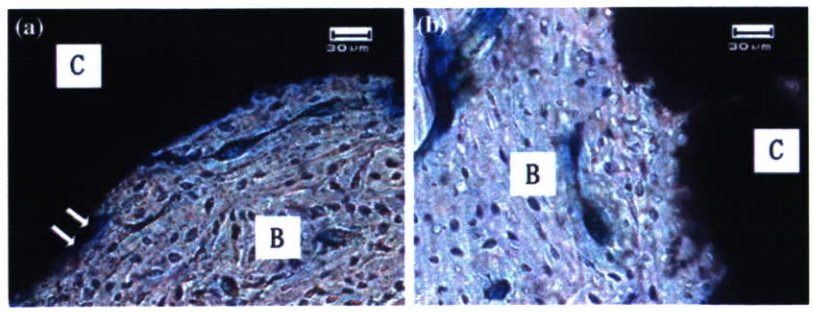

Fig. 5 Giemsa surface staining of (**a**) ST2-50c and (**b**) ST2-56c in rat tibiae 12 weeks after implantation. C, cement; B, bone; Arrows indicate intervening soft tissue. Bar = 30 μm

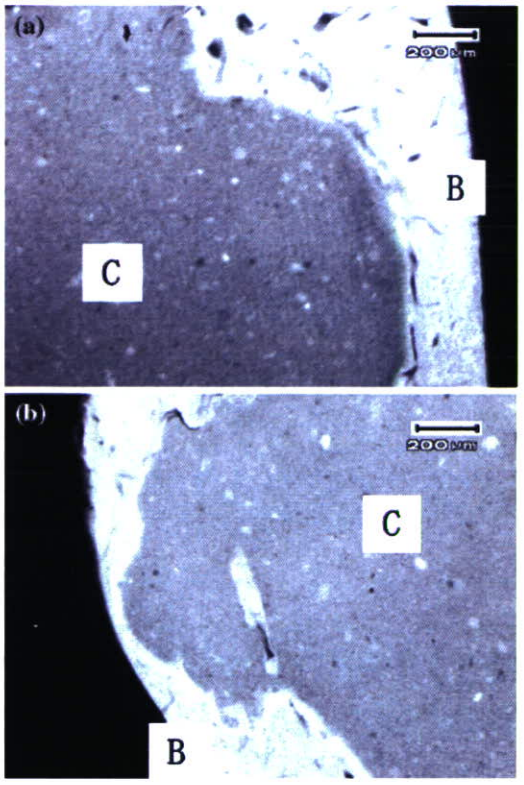

Fig. 7 Contact microradiography of (**a**) ST2-50c and (**b**) ST2-56c in rat tibiae 12 weeks after implantation. C, cement; B, bone. Bar = 200 μm

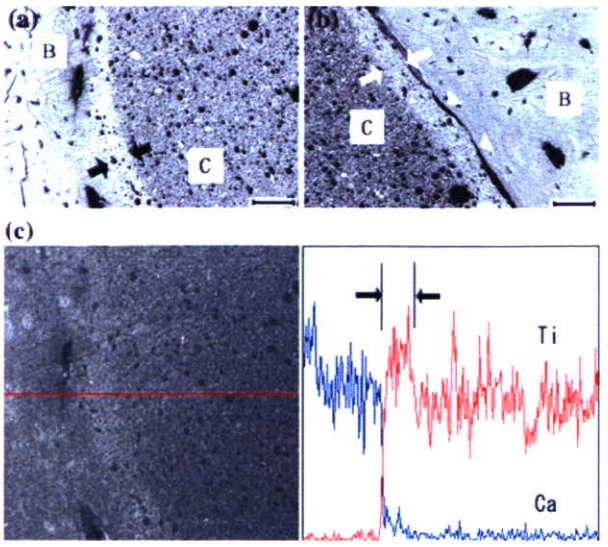

Fig. 8 Back-scattered scanning electron micrographs (SEM) of (**a**) ST2-56c and (**b**) ST2-50c in rat tibiae six weeks after implantation, and (**c**) SEM energy-dispersive X-ray (EDX) analysis of ST2-56c in the same site of (**a**). The white line is clearly visible in (**a**) and (**b**), and SEM–EDX analysis indicated that the white line is a Ti-rich layer. An increase of the intensity of the calcium peak was also detected along the outer margin of the white line. Arrowheads indicate thin intervening soft tissue. Between arrows = white line. C, cement; B, bone. Bar = 40 μm

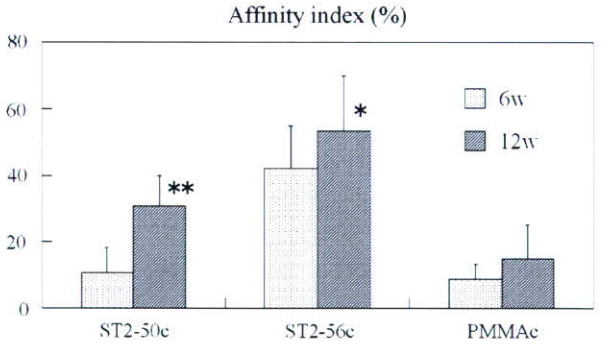

Fig. 9 Affinity indices (%) for ST2-50c, ST2-56c, and PMMAc in rat tibiae at six and 12 weeks after implantation (mean ± SD, n = 12). At six weeks, the value for ST2-50c was 10.6 ± 7.8 and 42.1 ± 12.9 for ST2-56c; and at 12 weeks, 30.8 ± 9.0 and 53.4 ± 16.6 respectively. The comparative affinity indices for PMMAc were 8.9 ± 4.4 and 14.9 ± 10.4 at six and 12 weeks, respectively [16]. *Significant compared with ST2-50c and PMMAc at six and 12 weeks. **Significant compared with PMMAc at 12 weeks

cement [10]. In contrast, micron-sized particles of mixed-phase anatase–rutile titania dispersed well in the cements, as was shown in this study. Indeed, it is difficult to simply compare the results of the experiments because there was little difference in the experimental conditions including the PMMA/MMA ratio and silanization of the powders. However, the difference in the particle size presumably influenced the degree of the particle dispersion.

The compressive and bending strengths of ST2-50c were much higher than those previously reported for PMMA-based composite cements containing nanosized spherical titania particles at 50 wt%, the compressive and bending strengths of which were 91.8 ± 7.7 and 25.5 ± 9.5 MPa, respectively [10]. Shinzato et al. developed PMMA-based composite cements containing glass beads and reported that a decreasing trend in the bending strength was observed as the glass bead size increased [16]. Their results suggest that cements containing smaller-sized titania could have higher strength. However, our findings were not consistent with theirs, and were presumably influenced mainly by the difference in filler dispersion in our studies, where the micron-sized titania dispersed well, whereas the nanosized titania used in the previous study formed some aggregates in the cement [10]. In this study, there was an increasing trend in compressive strength, bending strength, and bending modulus with increasing titania filler content. Juhasz et al. investigated the effect of filler content on the mechanical properties of AW-glass ceramic–polyethylene composites, and noted that a stiffening effect was observed as the AW-glass ceramic filler content increased from 10 to 50 vol% [17]. Their results were consistent with ours. In this study,

the mechanical strengths of the cements containing micron-sized titania particles met the criteria required by the ISO 5833 standard.

The setting times of the cements containing titania particles in this study were reduced, and the peak temperature decreased, as titania filler content increased. Only ST2-56c exhibited a lower peak temperature than PMMAc, and that of ST2-50c was almost the same as that of PMMAc. This was probably because the weight ratio of PMMA/MMA was 1/2 in ST2-50c, whereas the weight ratio of powder/liquid monomer was about 2/1 in PMMAc, and the content of MMA that polymerizes with an exothermic reaction was almost the same in ST2-50c and PMMAc. As less exothermic setting reactions for bone cement are desirable, both ST2-50c and ST2-56c would be acceptable, but ST2-56c appeared to have lower peak-setting temperature properties and is therefore recommended.

Animal experiments revealed that both ST2-50c and ST2-56c were more osteoconductive than cements containing nanosized titania particles. According to a previous study, the affinity indices of cements containing nanosized titania particles were 20.9 ± 7.3% for cement containing 50 wt% titania particles and 31.3 ± 8.7% for cement containing 60 wt% titania particles at 12 weeks [10]. In the previous study [10] and in this study, high molecular weight PMMA powder was used because it showed low solubility in the MMA monomer during the polymerizing reaction [14]. As a result, bioactive fillers could be exposed at the cement surface without being covered by a layer of polymerized MMA [14]. Therefore, the amount of bioactive particles exposed on the cement surface, which must be proportional to cement bioactivity, was greatly influenced by the particle size of bioactive fillers. In this study, the micron size of the titania particles presumably had a beneficial effect on the osteoconductivity of ST2-50c and ST2-56c. However, ST2-56c was in direct contact with bone over larger areas than ST2-50c, at both six and 12 weeks after implantation into rat tibiae. As well as the larger amount of titania filler, presumably the decrease in toxic monomer content contributed to the higher affinity indices of ST2-56c compared with those of ST2-50c. Further research on bone-bonding strength is necessary to demonstrate the bioactivity of ST2-50c and ST2-56c.

The marginal white line seen on SEM was a Ti-rich layer, as revealed by SEM–EDX analyses (Fig. 8c) and has been similarly observed in cements containing nanosized titania particles [10]. In contrast, it has been reported that PMMA-based composite cement containing glass beads, AW-GC, or hydroxyapatite fillers developed by Shinzato et al. exhibited no such marginal line, although they used a similar PMMA/MMA system and bioactive fillers silanized with γ-methacryloxypropyltrimethoxy silane [14]. Therefore, the properties of the titania filler itself are suggested to contribute to the formation of the white line. Because a Ti-rich layer indicated bioactive titania gathered at the cement surface, it presumably contributes to the osteoconductivity of cements containing titania particles. SEM–EDX analyses also revealed an increase in the concentration of calcium along the outer margin of the white line, which suggests calcium ion transfer or bony tissue invasion into the cement margin. Although a small amount of unpolymerized MMA might leak out of the cement surface, SEM observations revealed no such cement degradation and that leakage was minimal. No toxic effects of the monomer were detected by Giemsa surface staining, and excellent osteointegration of ST2-56c and ST2-50c was seen.

The overall results of this study indicate that PMMA bone cement containing micron-sized titania particles is a promising bone cement for prosthesis fixation as well as for vertebroplasty, but further research on long-term osteointegration and bone-bonding strength should be performed before clinical application.

Conclusions

Three types of PMMA-based composite cements containing 40–56 wt% micron-sized bioactive titania powder were prepared, and their mechanical, setting, and biological properties were evaluated. Compressive strength, bending strength, and bending modulus increased with increasing content of titania filler. The mechanical strengths met the criteria required in the ISO 5833 standard. The peak temperature during the setting reaction decreased as the amount of filler increased, and ST2-56c exhibited a lower peak temperature than commercial PMMA cement. Cements ST2-50c and ST2-56c were revealed to be biocompatible and osteoconductive. This was especially the case with ST2-56c, as it was in direct contact with bone over large areas within six weeks after implantation into rat tibiae, and showed significantly higher affinity indices than those of ST2-50c within 12 weeks. Overall, the data indicate that bone cement containing micron-sized titania particles can be applied to prosthesis fixation as well as vertebroplasty, and ST2-56c is a good candidate cement.

Acknowledgements We greatly appreciate the technical support of Makio Fujioka for the SEM studies.

References

1. S. M. KENNY and M. BUGGY, *J. Mater. Sci. Mater. Med.* **14** (2003) 923
2. M. A. FREEMAN, G. W. BRADLEY and P. A. REVEL, *J. Bone Joint Surg. Br.* **64** (1982) 489

3. S. R. GOLDRING, A. L. SCHILLER, M. ROELKE, C. M. ROURKE, D. A. O'NEIL and W. H. HARRIS, *J. Bone Joint Surg. Am.* **65** (1983) 575
4. F. M. KHAW, L. M. KIRK, R. W. MORRIS and P. J. GREGG, *J. Bone Joint Surg. Br.* **84** (2002) 658
5. J. J. CALLAGHAN, J. E. TEMPLETON, S. S. LIU, D. R. PEDERSEN, D. D. GOETZ, P. M. SULLIVAN and R. C. JOHNSTON, *J. Bone Joint Surg. Am.* **86-A** (2004) 690
6. M. UCHIDA, H. M. KIM, T. KOKUBO, S. FUJIBAYASHI and T. NAKAMURA, *J. Biomed. Mater. Res.* **64A** (2003) 164
7. M. UCHIDA, H. M. KIM, T. KOKUBO, S. FUJIBAYASHI and T. NAKAMURA, *J. Biomed. Mater. Res.* **63** (2002) 522
8. W. Q. YAN, T. NAKAMURA, M. KOBAYASHI, H. M. KIM, J. MIYAJI and T. KOKUBO, *J. Biomed. Mater. Res.* **37** (1997) 267
9. Y. T. SUL, *Biomaterials* **24** (2003) 3893
10. K. GOTO, J. TAMURA, S. SHINZATO, S. FUJIBAYASHI, M. HASHIMOTO, M. KAWASHITA, T. KOKUBO and T. NAKAMURA, *Biomaterials* **26** (2005) 6496
11. T. KOKUBO, S. ITO, Z. T. HUANG, T. HAYASHI, S. SAKKA, T. KITSUGI and T. YAMAMURO, *J. Biomed. Mater. Res.* **24** (1990) 331
12. S. SHINZATO, T. NAKAMURA, T. KOKUBO and Y. KITAMURA, *J. Biomed. Mater. Res.* **54** (2001) 491
13. T. NAKAMURA, H. KATO, Y. OKADA, S. SHINZATO, K. KAWANABE, J. TAMURA and T. KOKUBO, In *Bioceramics*, edited by S. Gianniniand A. Moroni (Bologna: Trans Tech, 2000), p. 661
14. S. SHINZATO, M. KOBAYASHI, W. F. MOUSA, M. KAMIMURA, M. NEO, Y. KITAMURA, T. KOKUBO and T. NAKAMURA, *J. Biomed. Mater. Res.* **51** (2000) 258
15. J. TAMURA, K. KAWANABE, T. YAMAMURO, T. NAKAMURA, T. KOKUBO, S. YOSHIHARA and T. SHIBUYA, *J. Biomed. Mater. Res.* **29** (1995) 551
16. S. SHINZATO, T. NAKAMURA, T. KOKUBO and Y. KITAMURA, *J. Biomed. Mater. Res.* **56** (2001) 452
17. J. A. JUHASZ, S. M. BEST, R. BROOKS, M. KAWASHITA, N. MIYATA, T. KOKUBO, T. NAKAMURA and W. BONFIELD, *Biomaterials* **25** (2004) 949

Enhanced Wear Resistance of Orthopaedic Bearing Due to the Cross-Linking of Poly(MPC) Graft Chains Induced by Gamma-Ray Irradiation

Masayuki Kyomoto,[1,2] Toru Moro,[3] Fumiaki Miyaji,[1] Tomohiro Konno,[2] Masami Hashimoto,[4] Hiroshi Kawaguchi,[3] Yoshio Takatori,[3] Kozo Nakamura,[3] Kazuhiko Ishihara[2]

[1] Research Division, Japan Medical Materials Corporation, Osaka, Japan

[2] Department of Materials Engineering, School of Engineering and Center for NanoBio Integration, The University of Tokyo, Tokyo, Japan

[3] Department of Orthopaedic Surgery, School of Medicine, The University of Tokyo, Tokyo, Japan

[4] Materials Research and Development Laboratory, Japan Fine Ceramics Center, Nagoya, Japan

Received 17 January 2007; revised 31 March 2007; accepted 30 April 2007
Published online 22 June 2007 in Wiley InterScience (www.interscience.wiley.com). DOI: 10.1002/jbm.b.30874

Abstract: We assumed that the extra energy supplied by gamma-ray irradiation produced cross-links in 2-methacryloyloxyethyl phosphorylcholine (MPC) polymer grafted cross-linked polyethylene (CLPE-*g*-MPC) and investigated its effects on the tribological properties of CLPE-*g*-MPC. In this study, we found that the gamma-ray irradiation produced cross-links in three kinds of regions of CLPE-*g*-MPC: poly(MPC) layer, CLPE-MPC interface, and CLPE substrate. The dynamic coefficient of friction of CLPE-*g*-MPC slightly increased with increasing irradiation doses. After the simulator test, both the nonsterilized and gamma-ray sterilized CLPE-*g*-MPC cups exhibited lower wear than the untreated CLPE ones. In particular, the gamma-ray sterilized CLPE-*g*-MPC cups showed extremely low and stable wear. As for the nonsterilized CLPE-*g*-MPC cups, the weight change varied with each cup. When the CLPE surface is modified by poly(MPC) grafting, the MPC graft polymer leads to a significant reduction in the sliding friction between the surfaces that are grafted because water thin films formed can behave as extremely efficient lubricants. Such a cross-link of poly(MPC) slightly increases the friction of CLPE by gamma-ray irradiation but provides a stable wear resistant layer on the friction surface. The cross-links formed by gamma-ray irradiation would give further longevity to the CLPE-*g*-MPC cups. © 2007 Wiley Periodicals, Inc. J Biomed Mater Res Part B: Appl Biomater 84B: 320–327, 2008

Keywords: joint replacements; polyethylene; phosphorylcholine; sterilization

INTRODUCTION

The number of primary and revised artificial hip and knee joints used are substantially increasing in the world every year.[1] This means that the quality of artificial joints has been becoming increasingly important. Most of the patients who receive an artificial joint experience a dramatic pain relief and enjoy a rapid improvement in the quality of life. The most popular artificial joint system is a bearing couple composed of an ultra-high molecular weight polyethylene (UHMWPE) and Co-Cr-Mo alloy. However, osteolysis caused by wear particles of UHMWPE has emerged as a serious issue.[2–4] The reduction in the number of UHMWPE wear particles is a method to prevent osteolysis. From this viewpoint, different combinations of bearing surfaces and improvement in the bearing materials have been focused upon.

We have recently developed a novel artificial joint system with 2-methacryloyloxyethyl phosphorylcholine (MPC) polymer grafted onto the surface of cross-linked polyethylene (CLPE-*g*-MPC),[5–7] aiming to reduce wear and avoid bone resorption. MPC is a methacrylate monomer that has a phospholipid polar group in a side chain and is used to make novel biomaterials as designed by Ishihara et al., who were inspired by the natural phospholipids of biomembranes.[8] MPC can be a good polymer biomaterial owing to

Correspondence to: M. Kyomoto (e-mail: kyomotom@jmmc.jp)
Contract grant sponsor: Japanese Ministry of Education, Culture, Sports, Science, and Technology; Contract grant number: 15390449
Contract grant sponsor: Japanese Ministry of Health, Labour, and Welfare

the reduction of protein adsorption and cell adhesion.[9–18] On the basis of the biocompatibility and hydrophilicity of MPC polymers, we have been developing new artificial joints with highly lubricated bearing surfaces that are produced by photo-induced radical graft polymerization.[19] This technique grafts MPC directly onto CLPE, forming C—C covalent bonds between the CLPE substrate and the MPC polymer.

Medical devices, including artificial joints, are normally sterilized by using several methods, for example, gamma-ray sterilization, ethylene oxide gas sterilization, and gas plasma sterilization. In particular, gamma-ray irradiation is the sterilization method typically used for the UHMWPE components of artificial joints. However, gamma-ray sterilization probably influences the properties of medical devices. Generally, when a high energy beam generated by gamma-ray sterilization is irradiated on to a polymer, free radicals are formed by the scission of the molecular chains. This is followed by the retermination and cross-linking of the molecules. The irradiation of high-dose gamma-rays onto UHMWPE severs the C—C or C—H bonds, and it then produces cross-linking and subsequent chemical bonding involving C=O and C—C.[20] It has been reported that gamma-ray sterilized UHMWPE sometimes exhibits improved wear resistance due to the formation of many cross-links. Several investigators have reported that wear resistance is better in gamma-ray sterilized UHMWPE than that in ethylene oxide sterilized UHMWPE.[21–24]

The purpose of this study is to investigate the dependence of gamma-ray irradiation on the tribological (friction and *in vitro* wear) properties of CLPE-*g*-MPC and to examine the possibility of controlling the longevity of artificial joints by using this material. This is based on the hypothesis that the extra energy supplied by gamma-ray irradiation could produce cross-links in CLPE-*g*-MPC.

MATERIALS AND METHODS

Chemicals and MPC Graft Polymerization

Benzophenone and acetone were purchased from Wako Pure Chemical Industries (Osaka, Japan). MPC was industrially synthesized using the method reported by Ishihara et al.[8] and was supplied by Ai Bio-Chips (Tokyo, Japan).

A compression-molded UHMWPE (GUR1020 resin, Poly Hi-Solidur, IN) bar stock was treated with a dose of 50 kGy gamma irradiation in N_2 gas and annealed at 120°C for 7.5 h in N_2 gas in order to attain cross-linking. The CLPE specimens were machined from this bar stock after cooling. They were immersed in an acetone solution containing 10 mg/mL benzophenone for 30 s and then dried in the dark at room temperature to remove acetone. The amount of benzophenone adsorbed on the surface was 3.5×10^{-11} mol/cm^2.[25] The MPC monomer was dissolved in pure degassed water up to a concentration of 0.5 mol/L. The CLPE specimens coated with benzophenone were immersed in the aqueous MPC solution. The photo-induced graft polymerization on the CLPE surface was carried out with an ultraviolet irradiation (UVL-400HA ultra-high pressure mercury lamp, Riko-Kagaku Sangyo, Funabashi, Japan) of 5 mW/cm^2 at 60°C for 90 min using a filter (Model D-35; Toshiba, Tokyo, Japan) to pass only ultraviolet light with a wavelength of 350 ± 50 nm. After the polymerization, the CLPE-*g*-MPC specimens were removed, washed with pure water and ethanol, and dried at room temperature. The CLPE and CLPE-*g*-MPC specimens were sterilized by gamma-ray irradiation of 25 or 50 kGy in N_2 gas.

Surface Analysis by Fourier-Transform Infrared and X-ray Photoelectron Spectroscopies and Water-Contact Angle Measurement

The functional group vibrations of both the nonsterilized and gamma-ray sterilized CLPE and CLPE-*g*-MPC surfaces were examined by Fourier-transform infrared (FTIR) spectroscopy using attenuated total reflection (ATR) equipment. The FTIR/ATR spectra were obtained in 32 scans over a range of 800–2000 cm^{-1} using an FTIR analyzer (FT/IR-615; JASCO International, Tokyo, Japan) at a resolution of 4.0 cm^{-1}.

The surface elemental conditions of CLPE before and after MPC grafting were analyzed by X-ray photoelectron spectroscopy (XPS). The XPS spectra were obtained using an XPS spectrophotometer (AXIS Hsi 165; Kratos Analytical, UK) equipped with an Mg-Kα radiation source at 15 kV at the anode. The take-off angle of the photoelectrons was kept at 90°. Each sample was scanned five times.

The static water-contact angles of CLPE-*g*-MPC with various photo-polymerization periods were measured by a sessile drop method using an optical bench-type contact angle goniometer (Model DM300; Kyowa Interface Science, Saitama, Japan). Drops of purified water (1 μL) were deposited onto the surface of CLPE-*g*-MPC, and the contact angles were directly measured by using a microscope after 60 s according to the ISO 15989 standard.[26] Fifteen replicate measurements were performed on each sample, and the average values were taken as contact angles.

Friction Test

The friction test was performed using a ball-on-plate machine (Tribostation 32; Shinto Scientific, Tokyo, Japan). Six sample pieces were prepared using each of the sterilization methods. The Co-Cr-Mo alloy ball was 9 mm in diameter and its surface roughness was Ra $\geq$ 0.01—as smooth as a femoral ball. The friction tests were carried out with a load of 0.98 N and a sliding distance of 25 mm with a frequency of 1 Hz at room temperature. The measurements were performed using pure water as lubricant. The friction tests were performed up to a maximum of 100 cycles. The mean static (μ_s) and dynamic (μ_d) coefficients of friction were determined by averaging five data points in 10 (8–12) and 100 (96–100) cycle measurements.

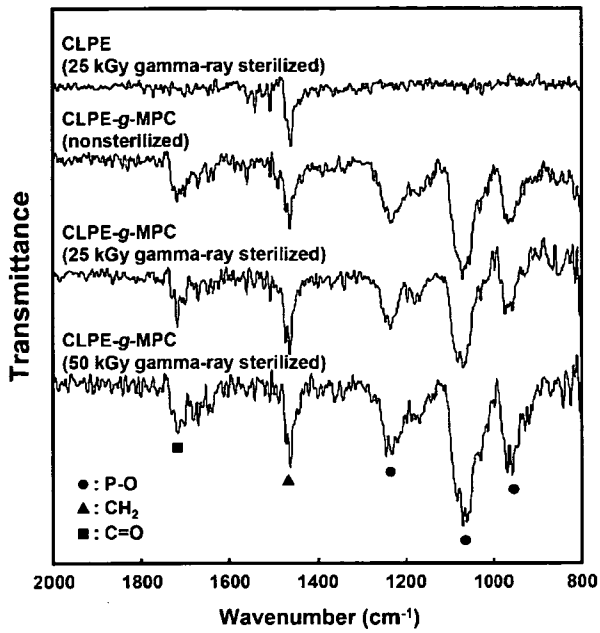

Figure 1. FTIR/ATR spectra for nonsterilized and gamma-ray sterilized CLPE and CLPE-*g*-MPC.

Statistical Analysis

For the water-contact angle measurement and friction test, the results derived from each measurement were expressed as mean values and the standard deviation. The statistical significance ($p < 0.05$) was judged by the Student's *t*-test.

Hip Joint Simulator Test

The inner and outer diameters of the CLPE and CLPE-*g*-MPC cups used in the hip joint simulator were 26 and 52 mm, respectively. Four pieces for each condition was prepared. The wear test was performed using a 12-station hip joint simulator (MTS Systems, MN). A Co-Cr-Mo alloy femoral ball component with a size of 26 mm (Japan Medical Materials, Osaka, Japan) was used as *a femoral* component. A mixture of 25 vol % bovine serum, 20 mM/L of ethylene diamine tetraacetic acid (EDTA), and 0.1 mass % sodium azide was used as lubricant, according to the ISO 14242-1 standard.[27] The lubricant was replaced every 0.5 $\times 10^6$ cycles. Loads simulating a physiologic loading curve with double peaks of 1793 and 2744 N loads were applied with a frequency of 1 Hz. The wear was determined by weighing the polyethylene cups. Load-soak controls ($n = 2$) were used to compensate the fluid absorption of specimens. The weights of the cups were measured every 0.5×10^6 cycles. Then, the testing was continued until a total of 5.0×10^6 cycles were completed.[28]

To evaluate the wear conditions, the surface features of the bearing surfaces of the cups were observed with a confocal laser scanning microscope (OLS1200; Olympus, Tokyo, Japan) after a simulator test with 5.0×10^6 cycles.

RESULTS

Figure 1 shows the FTIR/ATR spectra for the nonsterilized and gamma-ray sterilized CLPE and CLPE-*g*-MPC. An absorption peak was observed at 1460 cm^{-1} for both CLPE and CLPE-*g*-MPC. This peak is attributed mainly to the methylene chain in the CLPE substrate and MPC graft polymer. However, the transmission absorptions at 1240, 1080, and 970 cm^{-1} were observed only for the CLPE-*g*-MPC. These peaks are due to the phosphate group in the MPC unit. Similarly, an absorption peak at 1720 cm^{-1} observed for CLPE-*g*-MPC only corresponds to the carbonyl group in the MPC unit. The FTIR/ATR spectra did not differ significantly between the nonsterilized and gamma-ray sterilized CLPE-*g*-MPC.

Table I summarizes the elemental compositions of the untreated CLPE and the nonsterilized and gamma-ray sterilized CLPE-*g*-MPC surfaces. Both the elemental composition of nitrogen and phosphorous in the nonsterilized and gamma-ray sterilized CLPE-*g*-MPC surface were approximately 5.2. It should be noted that the contents of nitrogen and phosphorous in the CLPE-*g*-MPC surface remained unchanged after gamma-ray sterilization. The elemental composition of the CLPE-*g*-MPC surface was almost equivalent to the theoretical elemental composition (N = 5.3, P = 5.3) of poly(MPC). On the other hand, the carbon content in the gamma-ray sterilized CLPE-*g*-MPC slightly increased as compared with that of the nonsterilized one.

Figure 2 shows the static water-contact angle of the untreated CLPE and the nonsterilized and gamma-ray sterilized CLPE-*g*-MPC surfaces. The static water-contact angle

TABLE I. Surface Elemental Composition (%) of Gamma-Ray Sterilized CLPE and CLPE-*g*-MPC

Sample (Sterilization Method)	Surface Elemental Composition (%) (n = 5)			
	C	O	N	P
CLPE (nonsterilized)	99.8 (0.3)[a]	0.2 (0.3)	0.0 (0.0)	0.0 (0.0)
CLPE (25 kGy γ-sterilized)	99.5 (0.2)	0.6 (0.2)	0.0 (0.0)	0.0 (0.0)
CLPE (50 kGy γ-sterilized)	99.1 (0.2)	0.9 (0.2)	0.0 (0.0)	0.0 (0.0)
CLPE-*g*-MPC (nonsterilized)	58.0 (0.2)	31.5 (0.2)	5.2 (0.1)	5.3 (0.1)
CLPE-*g*-MPC (25 kGy γ-sterilized)	63.7 (2.3)	26.0 (2.3)	5.2 (0.1)	5.1 (0.2)
CLPE-*g*-MPC (50 kGy γ-sterilized)	65.0 (0.6)	24.6 (0.5)	5.2 (0.1)	5.2 (0.1)
MPC polymer[b]	57.9	31.6	5.3	5.3

[a] The standard deviation is in parentheses.
[b] Theoretical elemental composition of MPC polymer.

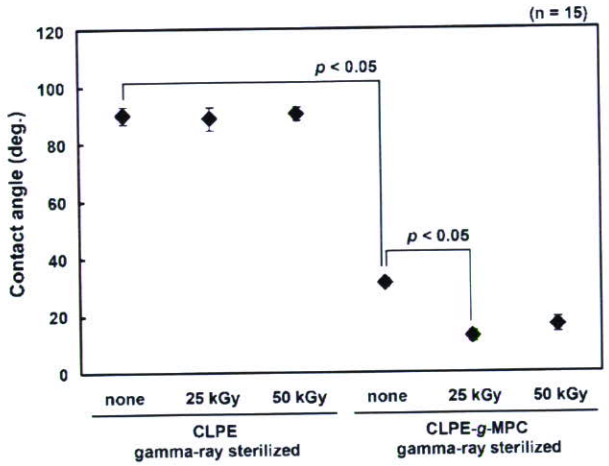

Figure 2. Static water-contact angle of the untreated CLPE and the nonsterilized and the gamma-ray sterilized CLPE-*g*-MPC surfaces. Bar; Standard deviations.

of the untreated CLPE was approximately 90° before and after gamma-ray sterilization, and it drastically decreased (approximately 30°) because of MPC grafting. Furthermore, the static water-contact angles of CLPE-*g*-MPC decreased to 15° after gamma-ray sterilization.

The static and dynamic coefficients of friction of gamma-ray sterilized CLPE and nonsterilized and gamma-ray sterilized CLPE-*g*-MPC are shown in Figures 3 and 4. Both the static and dynamic coefficients of friction of CLPE-*g*-MPC decreased drastically when compared with those of untreated CLPE. The degree of reduction in the coefficient was larger in the latter as compared to the former. Considering the gamma-ray sterilized CLPE-*g*-MPC, regardless of the dose of the gamma-ray sterilization and the cycles, approximately 50% reduction (i.e., 46–65%) was observed in the static coefficients of friction for both the 10 and 100 cycles when compared with those of untreated CLPE. On the other hand, the dose of gamma-ray sterilization affected the dynamic coefficient of friction of CLPE-*g*-MPC. That is, it slightly increased from 0.007 (none) to 0.021 (50 kGy) with an increase in the gamma-ray sterilization dose for 10 cycles. The dynamic coefficient of friction of CLPE-*g*-MPC with gamma-ray sterilization of 50 kGy was 75% greater ($p < 0.05$) than that of CLPE-*g*-MPC with nonsterilization.

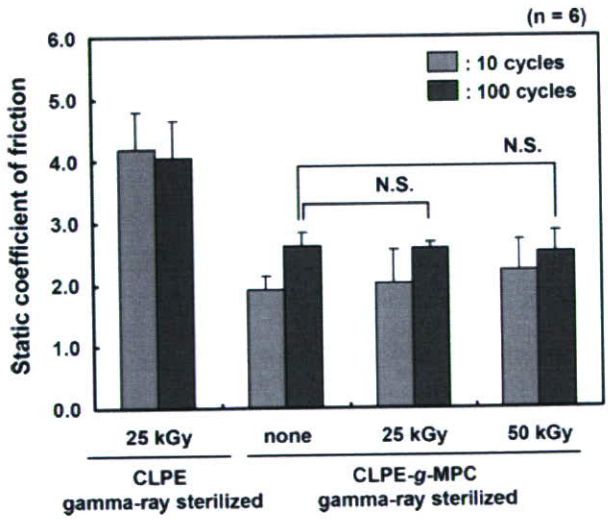

Figure 3. Static coefficients of friction of the gamma-ray sterilized CLPE surfaces and nonsterilized and gamma-ray sterilized CLPE-*g*-MPC surfaces. Bar; Standard deviations.

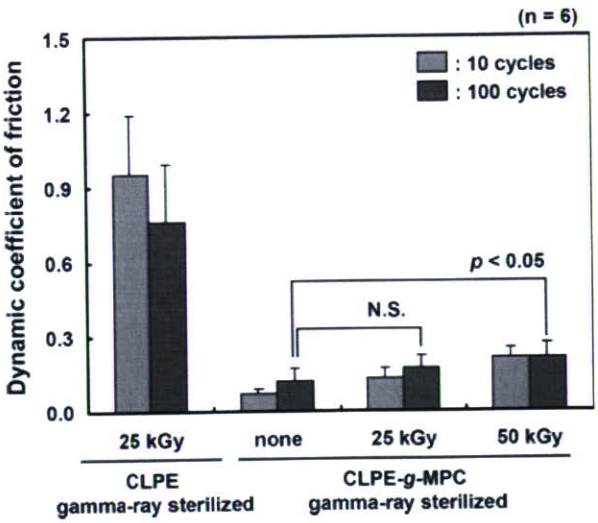

Figure 4. Dynamic coefficients of friction of gamma-ray sterilized CLPE surfaces and nonsterilized and gamma-ray sterilized CLPE-*g*-MPC surfaces. Bar; Standard deviations.

Figure 5 shows the weight change (gravimetric wear) of the gamma-ray sterilized CLPE cups and nonsterilized and gamma-ray sterilized CLPE-*g*-MPC cups in the hip joint simulation test. When the gravimetric method is used, the weight loss was corrected for the fluid absorption by sub-

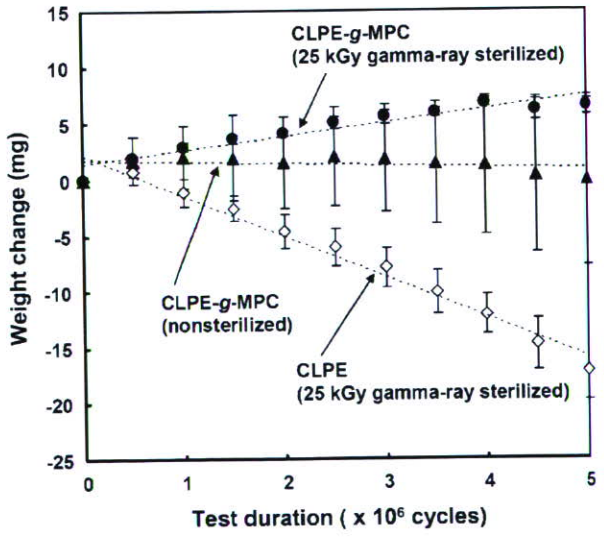

Figure 5. Weight change (gravimetric wear) of gamma-ray sterilized CLPE cups and nonsterilized and gamma-ray sterilized CLPE-*g*-MPC cups in the hip joint simulation test. Bar; Standard deviations.

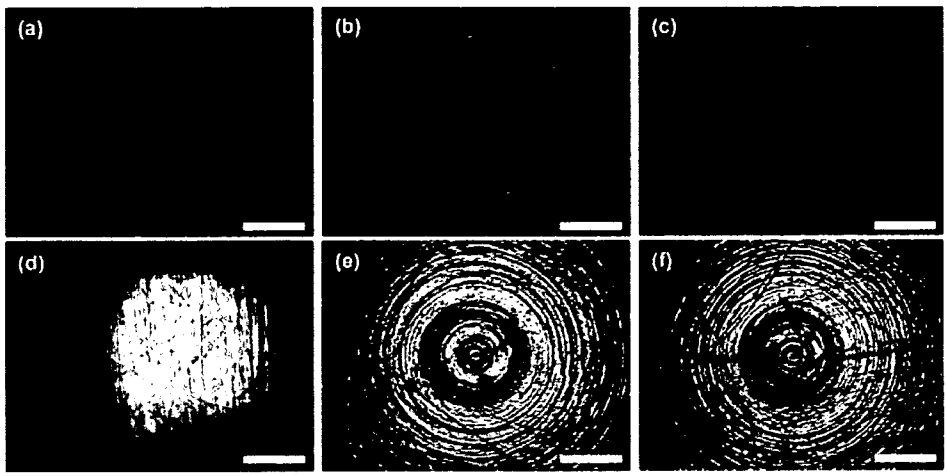

Figure 6. Confocal laser scanning microscope images of the CLPE and CLPE-*g*-MPC bearing surfaces before and after the hip simulator test. (a) CLPE (gamma-ray sterilized), (b) CLPE-*g*-MPC (nonsterilized), (c) CLPE-*g*-MPC (gamma-ray sterilized) before the hip simulator test, (d) CLPE (gamma-ray sterilized), (e) CLPE-*g*-MPC (nonsterilized), and (f) CLPE-*g*-MPC (gamma-ray sterilized) after the hip simulator test. The bar indicates 500 μm.

tracting the weight gain that occurred in the load-soak controls. Since the tested cups are subjected to a motion and load, such a "load-soak" correction is not necessarily satisfactory. Therefore, the tested cups absorb slightly more fluid than their load-soak controls. Consequently, the correction for using the load-soak control data may result in a slight underestimation of the actual weight loss. After 5.0 $\times$ 10^6 cycles of the simulator test, both the CLPE-*g*-MPC cups were found to undergo lesser wear than the untreated CLPE cups. In particular, the gamma-ray sterilized CLPE-*g*-MPC cups showed extremely low and stable wear. As for the nonsterilized CLPE-*g*-MPC cups, the weight change varied for each cup (standard deviation = 7.6 mg, n = 4). Figure 5 indicates that certain gamma-ray sterilized CLPE-*g*-MPC cups exhibit a slight increase in weight because of slightly enhanced fluid absorption when compared with that in the load-soak controls.

Figure 6 shows the confocal laser scanning microscope images of the bearing surfaces of the untreated gamma-ray sterilized CLPE cups and nonsterilized and gamma-ray sterilized CLPE-*g*-MPC cups before and after the simulator test. Before the simulator test, regular circular machining marks were seen on the all the bearing surfaces of the CLPE and CLPE-*g*-MPC cups. After the simulator test, the machining marks on these surfaces of the CLPE cups disappeared completely. On the contrary, clear machining marks with regular circles were observed on the surface of the nonsterilized and gamma-ray sterilized CLPE-*g*-MPC cups, indicating almost no wear on the surface.

DISCUSSION

We have developed an artificial hip joint using CLPE-*g*-MPC on the bearing surface with an objective of reducing wear and avoiding bone resorption. The static and dynamic coefficients of friction of CLPE-*g*-MPC reduced by >50% and >90%, respectively, as compared to those of the untreated CLPE, as shown in Figures 3 and 4. These friction coefficients were much lower than those usually found for the measurable shear interactions between UHMWPE and the Co-Cr-Mo alloy.[29,30] The significant reduction in the coefficients of friction of the grafted MPC polymer resulted in a substantial improvement in wear resistance, as shown in Figure 5. We assumed that the bearing surface of the artificial hip joint combined with the MPC polymer layer 100–200 nm thick exhibited the fluid film lubrication (or mixed lubrication) of the intermediate hydrated layer.[5,7,19]

These sterilizations may affect the properties of medical devices. Generally, when a high energy beam by gamma-ray sterilization is irradiated on a polymer, free radicals are formed by the scission of molecular chains.[20] This is followed by the retermination and cross-linking of the molecules. In this study, we therefore assumed that the extra energy supplied by gamma-ray irradiation produced cross-links in three kinds of regions of the CLPE-*g*-MPC: poly (MPC) layer, CLPE-MPC interface, and CLPE substrate, as shown in Figure 7.

As shown in Table I, the contents of nitrogen and phosphorous in the CLPE-*g*-MPC surface were hardly different between the nonsterilized CLPE-*g*-MPC and the gamma-ray sterilized CLPE-*g*-MPC. On the other hand, the contents of carbon and oxygen of CLPE-*g*-MPC slightly increased and decreased (as a trade-off), respectively, with an increase in the gamma-ray irradiation dose. It was assumed that the energy by gamma-ray irradiation would be used in the scission of C=O in the MPC structure by the degassing of O_2 and subsequently produce cross-links of poly(MPC) with chemical bonding involving C—C.[31,32] The extra energy supplied by gamma-ray sterilization of 25–50 kGy is clearly responsible for producing more cross-links.